

ON THE MULTILAMINATE MODELLING OF SOFT CLAYS

Kien Dang, Graduate Student, McGill University, Montreal, Quebec.

Mohamed A. Meguid, Assistant Professor, McGill University, Montreal, Quebec.

ABSTRACT

This paper describes a constitutive model for anisotropic clayey soils based on the multilaminate framework. The presented version of the model is suitable for the analysis of boundary value problems under unloading or loading conditions. The concepts of contact sampling planes and microstructure tensor are also discussed. The model is implemented into the software package (PLAXIS). Benchmarking against some of the well know constitutive models is presented.

RÉSUMÉ

Cet article décrit un modèle constitutif pour sols argileux anisotropes basés sur le cadre multilaminé. La version présente du modèle convient à l'analyse de problèmes à valeur de limites dans des conditions de charge ou de décharge. Les concepts de plans de prélèvement de contact et de tenseur de microstructure sont également discutés. Le modèle est mis en application dans le logiciel (PLAXIS). Un benchmarking avec certains des modèles constitutifs bien connus est présenté.

1. INTRODUCTION

Constitutive models that account for all known characteristics of soil behaviour (e.g. strength anisotropy, rotation of principal stresses, bonding effects, viscous effects, etc.) are difficult to use. A relevant model is usually employed to solve a given practical geotechnical problem. Among these soil characteristics, the strength anisotropy and rotation of principal stresses are known to have a significant effect on the modelling of geotechnical problems.

The Critical State model developed at Cambridge (Wood 1990) for normally consolidated and lightly overconsolidated clays is an isotropic hardening model and does not account for the rotation of principal stresses. Anisotropic hardening models (e.g. Wood and Graham 1990, Dafalias and Manzari 2002) do account for the rotation of principal stresses through a transitional rule described for the yield surface. However, the parameters of these models are based on tests in which no rotation of principal stresses takes place (Pande and Sharma 1983).

Several constitutive models have been developed in the past two decades to capture specific characteristics of soft clays. Wood and Graham (1990), Dafalias and Manzari (2002) modified the well-known Modified Cam Clay (MCC) to account for the anisotropic elasticity and reconstructed the yield loci to match the experimental observations. These models do not account for the strength anisotropy of the clay material. Kumbhojkar and Banerjee (1993) employed the plastic strains as a hardening parameter rather than the volumetric strain; however, the results did not match well with the experiment data. Furthermore, the model is complicated due to the large number of parameters required to define the yield surface. Another model that accounts for the undrained shear strength anisotropy is developed by Su and Liao (1998). The model was used to investigate the effect of principal stress orientation on the behaviour of saturated clays. The

model parameters required two specific tests, namely, CK_{oUC} and CK_{oUB} triaxial tests. The suitability of this criterion to model soft clays has been proven to be limited. Further development was introduced by Sun and Matsuka (2003). They modified the anisotropic hardening elastoplastic model for clays which is based on the MCC.

A multilaminate framework for modelling soft clay has been introduced by Pande and Sharma (1983). Extensions to the model have been presented by several authors (e.g. Pietruszczak and Pande, 2001, Cudny and Vermeer 2004, Wiltafsky *et al.* 2002, Schuller and Schweiger 2002) to model the inherent anisotropy and destructuration of soft clays. A brief overview of the multilaminate concept is provided in the following section.

2. OVERVIEW

2.1 The multilaminate concept

The concept of multilaminate modelling is based on intersecting a solid block of homogenous, isotropic, elastic material with an infinite number of randomly oriented planes (Pande and Sharma 1983). These planes render the solid block into an assemblage of perfectly-fitting polyhedral blocks (Figure 1) which have rough surfaces behaving in elasto/visco-plastic manner. It is assumed that the overall deformational behaviour of the clay can be obtained by evaluating the deformations along these planes under the current effective normal and shear stresses (σ_n , τ). The opening/closing of the inter-boundary gap (void ratio) in relation to the initial gap (initial void ratio) is a contributing factor in evaluating deformations. It is also assumed that all contact boundaries have the same characteristics in sliding with no interaction between them.

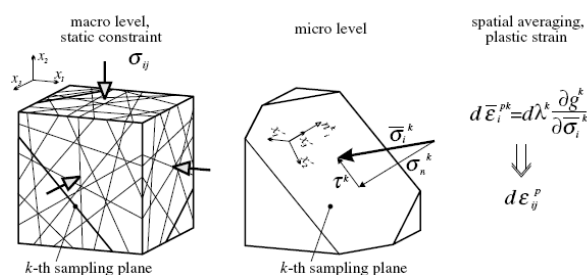


Figure 1. Schematic description of the multilaminate framework (Cudny and Vermeer 2003)

Another way of describing the multilaminate concept is by considering a load applied to a soil mass developing contact forces (of normal and tangential components) between adjacent particles. The overall deformational behaviour of the soil results from both deformation of individual particles and relative sliding between the particles. The latter is the major contribution to the overall strain and is accounted for in the multilaminate framework. Since the soil particles cannot be explicitly modelled, the interactions between them are considered in an averaged form of contact planes. The number, direction and orientation of the planes are governed by the integration rules. This means that individual planes do not interact and usually the same mathematical relations hold for all planes. However, this assumption is not strictly required and initial anisotropy may be easily introduced by varying parameter over the planes prior to loading (Schuller and Schweiger, 2002).

Since the introduction of the multilaminate framework for the analysis of clayey soils in 1983, several improvements and extensions were introduced. A multilaminate plasticity formulation was presented by Pietruszczak and Pande (1987) to account for the volumetric and deviatoric hardening of soils. Kartusen (1999) incorporated the deviatoric hardening and non-associated flow rule in their multilaminate formulation. The model was used to simulate the shear band formation in NATM tunnelling (Schuller and Schweiger 2002). Wiltafsky *et al.* (2002) presented a formulation employing the double hardening and volumetric hardening rules. A new version of the multilaminate model was presented by Cudny and Vermeer (2004) to account for the anisotropy and destructuration of soft clay.

2.2 Sampling planes

As discussed earlier, the concept of sampling planes is important in the formulation of multilaminate-based constitutive models. Loading imposed on clay blocks results in plastic strains developing along these contact planes. Contribution of plastic strain from all planes is spatially averaged to obtain the plastic increment of the macro strain tensor

$$d\epsilon^p = \sum_{i=1}^{\infty} d\epsilon^{pk} \quad (1)$$

In the numerical implementation, this averaging of infinite number of planes is not impossible but it requires a large amount of computation. Therefore, some integration rules are needed. Pande *et al.* (1987, 1994) proposed a 13-planes integration rule for 3D analyses and 9-planes integration rule for plane strain. Due to the development in computer technology, higher order integration rules are feasible today. An integration rule employing 64 contact planes is used by Cudny and Vermeer (2004). Recently, 2*33-planes integration rule has been used by Scharinger and Schweiger (2005).

The most important advantage of the multilaminate framework is the simplicity of formulation – standard isotropic elastic-plastic models can be easily converted to a multi-laminate version without introducing any new material parameters. The constitutive equation in the spatial coordinate reduces into the normal and shear stress acting on the considered plane.

2.3 Soil anisotropy

Strength anisotropy of the soil was not taken into account in the early development of the multilaminate framework, (Pande and Sharma (1982), Pande and Yamada (1994)). However, stress-induced anisotropy was considered by setting the initial anisotropic stress condition (K_0). This means that initial values of preconsolidation stress will be different on every sampling plane. As indicated by Cudny and Vermeer (2004), the degree of anisotropy gained from the initialization of the K_0 stress state, in most cases, was found to be too small compared with experimental results.

A formulation that accounts for the soil strength anisotropy was introduced by Pietruszczak and Mroz (2000). Strength parameters such as friction angle and cohesion were distributed directionally employing a microstructure tensor. Cudny and Vermeer (2004) indicated that for material like soft clays, it is more reasonable to distribute the overconsolidation ratio that is directly related to the bonding of soil fabric reach a good agreement with the critical state model. In this case, only the initial state variable is distributed directionally and changes during the process of straining. Relevant mathematical formulation required to model the strength anisotropy are described below.

Microstructure tensor, a_{ij} , represents a measure of the material fabric associated with the arrangement of intergranular contact. The principal triad of a_{ij} is specified by the unit vectors $e^{(\alpha)}$, $\alpha = 1, 2, 3$, so that the spectral decomposition of a_{ij} becomes

$$a_{ij} = a_1 e_i^{(1)} e_j^{(1)} + a_2 e_i^{(2)} e_j^{(2)} + a_3 e_i^{(3)} e_j^{(3)} \quad (2)$$

Where, a_1, a_2, a_3 are the principal values of the microstructure tensors and e_i and e_j are the respective structure-orientation tensors.

Considering the principal directions of the microstructure stress tensor and specifying the traction modulus on the

planes normal to principal axes (Figure 2). The magnitudes of the traction modulus are:

$$\begin{aligned} L_1 &= \sigma_{11}^2 + \sigma_{12}^2 + \sigma_{13}^2 \\ L_2 &= \sigma_{21}^2 + \sigma_{22}^2 + \sigma_{23}^2 \\ L_3 &= \sigma_{31}^2 + \sigma_{32}^2 + \sigma_{33}^2 \end{aligned} \quad (3)$$

Considering the general loading vector

$$L_i = L_1 e_i^{(1)} + L_2 e_i^{(2)} + L_3 e_i^{(3)} \quad (4)$$

The unit specifying the loading direction can be defined as

$$l_i = \frac{L_i}{(L_k L_k)^{1/2}} \quad (5)$$

The directional distribution of the scalar parameter α is obtained using an isotropic value α_0 as follows

$$\alpha = \alpha_0 (1 + \Omega_{ij} l_i l_j) \quad (6)$$

where a deviatoric measure of the material microstructure Ω is defined as

$$\Omega_{ij} = (a_{ij} - \frac{1}{3} \delta_{ij} a_{kk}) / (\frac{1}{3} a_{kk}) \quad (7)$$

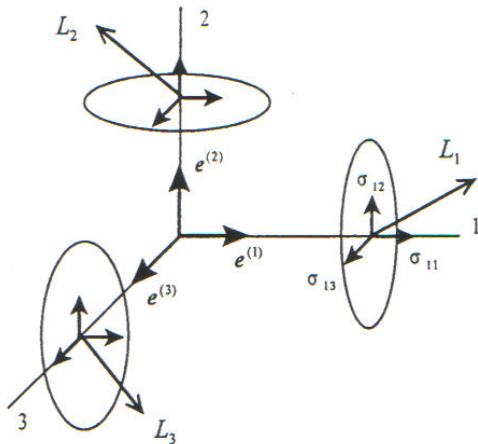


Figure 2. Principal triad of the micro structure tensor \mathbf{a} and the traction modulus L_1, L_2, L_3 . (Pietruszczak and Mroz, 2000)

2.4 Bonding and destructuration affect

Leroueil (1979) introduced the term “destructuration” to present the post-yield disruption of the natural structure of clays. Burland (1990) characterized the structure of natural clays by:

- The “fabric” consists of the spatial arrangement of soil particles and inter-particle contacts.
- “Bonding” between particles can be destroyed during plastic straining.

The existence of the inter-particle bonding provides additional resistance to yielding of soil. Lerouiel and Vaughan (1990) shown that the affect of bonding and destructuration is similar in most natural geological

material as well as in artificially cemented and grouted soil. Gens and Nova (1993) presented a general framework for incorporating bonding and destructuration within the elasto-plastic constitutive models. Beyond the real yield surface, an “intrinsic yield surface” is introduced to present the size of the yield surface with no bonding (Wheeler, Cudny and Wiltafsky, 2003). The difference in size of the real yield surface and the intrinsic yield surface is a measure of the bonding affect.

Cudny and Vemeer (2004) incorporated the influence of bonding and destructuration using the approach of Gens and Nova (1993). The mean value of bonding parameter x varied on each sampling plane.

3. MULTILAMINATE CONSITUTIVE MODEL

3.1 Elastic behaviour

The fabric anisotropy of clays influences both elastic and plastic behaviour. For normally and slightly overconsolidated clay, plastic strains dominate the contribution of anisotropy; moreover, elastic strain often plays an unimportant role (Wheeler, Cudny, Neher, Wiltafsky 2003). Considering anisotropy in elastic behaviour requires complex additional parameters. Therefore, elastic strain will be calculated at the macro level in this formulation. The relationship between stress and strain increments is:

$$d\sigma_{ij} = D_{ijkl}^e d\epsilon_{kl}^e$$

where D^e is the elastic stiffness. The hypoelastic stiffness based on Hooke’s law (often used in critical state models) was chosen in the present study.

For primary loading

$$D_{ijkl}^e = \frac{E(p)}{(1+\nu)(1-2\nu)} [\nu \delta_{ij} \delta_{kl} + \frac{1-2\nu}{2} (\delta_{ik} \delta_{jl} + \delta_{jk} \delta_{il})] \quad (8)$$

where

- ν is Poisson ratio
- $E(p)$ is pressure dependent Young modulus defined as
$$E(p) = \frac{3p(1-2\nu)}{\lambda^*}$$
- λ^* is the modified compression index estimated from $\ln p - \epsilon_v$ diagrams.

For unloading and reloading

$$D_{ijkl}^e = \frac{E(p)}{(1+\nu_{ur})(1-2\nu)} [\nu_{ur} \delta_{ij} \delta_{kl} + \frac{1-2\nu}{2} (\delta_{ik} \delta_{jl} + \delta_{jk} \delta_{il})]$$

where ν_{ur} is Poisson ratio
 $E(p)$ is pressure dependent Young modulus defined as

$$E(p) = \frac{3p(1-2\nu_{ur})}{\kappa^*}$$

κ^* is the modified swelling index estimated from $\ln p$ - ε_v diagrams.

The unload-reloading parameters are very important in tunnel modelling since the soil around tunnel being excavated is under unloading condition.

In order to determine the global plastic strain, $d\varepsilon^p$, using integration of the micro plastic strain, $d\varepsilon^{pk}$, is carried out on each sampling plane. In the case of elastic, isotropic material, the stiffness has the same component on every plane. Elastic relationship between increments of micro stress and strain vector on the sampling plane is of the form:

$$d\sigma_i^k = D_{ij}^{ek} d\varepsilon_j^{ek} \quad (9)$$

or in a matrix form:

$$\begin{bmatrix} d\sigma_1^k \\ d\sigma_2^k \\ d\sigma_3^k \end{bmatrix} = \begin{bmatrix} D_{3131}^{ek} & 0 & 0 \\ 0 & D_{2323}^{ek} & 0 \\ 0 & 0 & D_{3323}^{ek} \end{bmatrix} \begin{bmatrix} d\varepsilon_1^{ek} \\ d\varepsilon_2^{ek} \\ d\varepsilon_3^{ek} \end{bmatrix} \quad (10)$$

where

$$D_{3131}^{ek} = D_{3232}^{ek} = \frac{1}{1+\nu} E(p)$$

$$D_{3333}^{ek} = \frac{1-\nu}{(1-2\nu)(1+\nu)} E(p)$$

Micro stress increments $d\sigma_1, d\sigma_2, d\sigma_3$ and micro strain increments $d\varepsilon_1, d\varepsilon_2, d\varepsilon_3$ will be discussed in more details the next section.

3.2 Sampling planes

As mentioned above, the solution of equation (1) can be obtained using numerical integration rules. The higher the number of planes, the accurate calculated response. In this study, an integration rule with 64 sampling planes was used (see figure 3). This integration has been successfully used by other researchers (e.g. Schuller and Schweiger (2002) and Cudny and Vemeer (2004)).

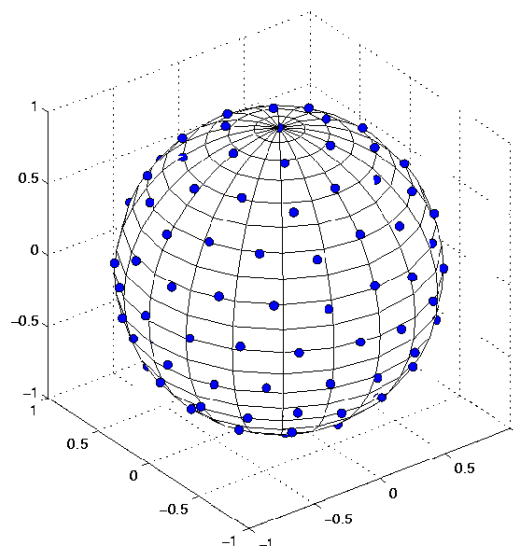


Figure 3. Integration note for a sphere (Fliege J and Maier U.1996)

The micro stress acting on each plane can be obtained using the auxiliary local coordinate system with orthogonal unit vector $x^{(k(1))}, x^{(k(2))}, x^{(k(3))} = n^k$.

$$\sigma_{ij}^k = D^k \cdot \sigma \cdot D^{kT} \quad (13)$$

where D is the matrix of directional cosines

$$D^k = \begin{bmatrix} x_1^{k(1)} & x_2^{k(1)} & x_3^{k(1)} \\ x_1^{k(2)} & x_2^{k(2)} & x_3^{k(2)} \\ x_1^{k(3)} & x_2^{k(3)} & x_3^{k(3)} \end{bmatrix}$$

Unit vectors $x^{k(1)}, x^{k(2)}$ are chosen arbitrarily in the sampling plane. It is common to select $x^{k(1)}$ first perpendicular to one of the normal vectors n^k and the remaining vectors can be calculated as a product of n^k and $x^{k(2)}$. Stress components can be calculated as follows:

$$\sigma_1^k = \sigma_{13}^k; \sigma_2^k = \sigma_{23}^k; \sigma_3^k = \sigma_{33}^k$$

Using the properties of the vector σ , a transform matrix (3 x 6) can be used to transform the macro stresses to micro stresses acting on each sampling plane

$$\bar{\sigma}_i^k = T_{ij}^{\sigma k} \bar{\sigma}_j, j=1..6 \quad (14)$$

where

$$T^{\sigma k} = \begin{bmatrix} (x_1^{k(1)})^2 & (x_2^{k(1)})^2 & (x_3^{k(1)})^2 & 2x_1^{k(1)}x_2^{k(1)} & 2x_2^{k(1)}x_3^{k(1)} & 2x_1^{k(1)}x_3^{k(1)} \\ (x_1^{k(2)})^2 & (x_2^{k(2)})^2 & (x_3^{k(2)})^2 & 2x_1^{k(2)}x_2^{k(2)} & 2x_2^{k(2)}x_3^{k(2)} & 2x_1^{k(2)}x_3^{k(2)} \\ (n_1^k)^2 & (n_2^k)^2 & (n_3^k)^2 & 2n_1^kn_2^k & 2n_2^kn_3^k & 2n_1^kn_3^k \end{bmatrix}$$

The back transformation process of the resulting increment of the micro plastic strain $d\varepsilon^{pk}$ is based on a spatial summation rule. Equation (1) can be substituted by the integration over the surface of sphere with a unit area with the assumption that the distribution of sampling planes is continuous.

$$d\varepsilon^p = \int_S d\varepsilon^{pk} dS \quad (15)$$

Equation (15) can be calculated by a numerical integration with a chosen scheme of sampling plane. The global plastic strain increment can be written as

$$d\varepsilon^p = \sum_{k=1}^m T_{ij}^{\varepsilon k} d\varepsilon_j^{pk} w_k = \sum_{k=1}^m d\lambda^k T_{ij}^{\varepsilon k} \frac{\partial g^k}{\partial \sigma_j^k} w_k, \quad i=1, \dots, 6 \quad (16)$$

where

w_k is the weight coefficient of k th plane in integration rule

$d\lambda^k$ is the plastic multiplier of k th plane

g is the potential function on the k th plane

The transformation matrix from the micro plastic strain increment to the global plastic strain increment $T^{\varepsilon k}$ is calculated similar to $T^{\sigma k}$ but based on the transpose matrix D^{kT}

$$\varepsilon_{ij}^k = D^{kT} \cdot \sigma \cdot D^k \quad (17)$$

It is beneficial to realize that $T^{\varepsilon k} = T^{\sigma kT}$

3.3 Microstructure tensor

To model the structural cross-anisotropy, the microstructure tensor, Ω , is used. One parameter Ω_v which defines the spatial bias of cross-anisotropic microstructure is needed

$$\Omega_{ij} = \begin{bmatrix} -\Omega_v/2 & 0 & 0 \\ 0 & \Omega_v & 0 \\ 0 & 0 & -\Omega_v/2 \end{bmatrix} \quad (11)$$

The directional attribution from equation (6) can be written as:

$$\alpha = \alpha_o (1 + \Omega_{ij} l_i l_j) = \alpha_o (1 + \Omega_{ij} n_i^k n_j^k) = \alpha_o (1 - \frac{\Omega_v}{2} (n_2^k)^2) \quad (12)$$

where n^k is the unit vector normal to the k^{th} sampling plane.

3.4 Yield surface and potential function

One of the advantages of the multi-laminate framework is its simplicity. The isotropic constitutive relation on each of the sampling plane can be expressed by using only one

micro stress invariant. An anisotropic behaviour on the macro level is simulated using spatial integration.

The micro yield surface, shown in Figure 4, consists of two parts: a cone and a cap which are responsible for shear and compressive strengths, respectively.

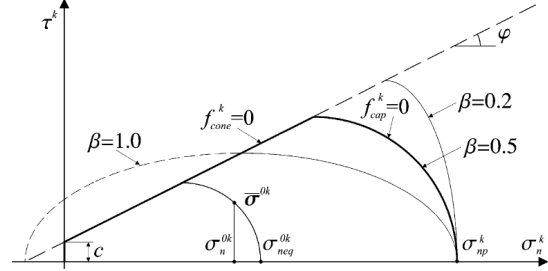


Figure 4. Yield surface on sampling plane (Cudny and Vermeer 2004)

The conical portion follows Mohr-Coulomb with non-associated flow rule. The yield and plastic potential functions are defined as (Duncan 1972)

$$f_{cone}^k = \tau^k - \sigma_n^k \mu - c \quad (18)$$

$$g_{cone}^k = \tau^k - \sigma_n^k \tan \psi \quad (19)$$

Where, $\mu = \tan \phi$ and ϕ, c, ω are the effective friction angle, effective cohesion, and dilatancy angle, respectively.

The cap part of the yield surface is based on MCC model (Cudny and Vermeer 2003) which accounts for the bonding affect of clays. This model takes the anisotropic behaviour into account by employing the microstructure tensor.

The yield function of the cap part can be written as:

$$f_{cap}^k = (\sigma_n^k - \sigma_{np}^k) \mu^2 \left[\frac{2\beta c}{\mu} + (1 + \beta) \sigma_n^k + (-1 + \beta) \sigma_{np}^k \right] + (\tau^k \beta)^2 (1 + \beta) = 0 \quad (20)$$

Where, σ_{np}^k is a micro preconsolidation pressure, and β is an additional parameter that controls the steepness of the cap surface. This parameter allows the influence of the asymptotic value of K_0^{nc} based on oedometer tests. For $\beta = 1$, the cap surface coincides with the MCC.

The preconsolidation pressure is calculated by the equation (based on Nova and Gens framework, 1993):

$$\sigma_{np}^k = \sigma_{neq}^{0k} (1 + b_0^k), \quad b_0^k = b_0 (1 + \Omega_v (n_2^k)^2) \quad (21)$$

Where, b_0 is isotropic or average bonding parameter

$$\sigma_{neq}^{0k} = \frac{\sigma_n^{0k} - \frac{\beta}{\mu} [-c + \sqrt{(c + \sigma_n^{0k} \mu)^2 + (-1 + \beta^2)(\tau^{0k})^2}]}{1 - \beta}$$

or
$$\sigma_{neq}^{0k} = \sigma_n^{0k} + \frac{(\tau^{0k})^2}{\mu(c + \sigma_n^{0k} \mu)} \text{ for } \beta = 1$$

3.5 Hardening rule

For the unbounded hardening component, the standard law for normally consolidated clay is employed:

$$\sigma_{np}^{*k} = \sigma_{np}^{0k} \exp\left(\frac{\varepsilon_n^{pk}}{\lambda^* - \kappa^*}\right) \quad (22)$$

Where, ε_n^{pk} is the normal invariant of plastic micro strain and λ^* and κ^* are compression and swelling indices, respectively, and can be estimated using $\ln(p)$ - ε_v diagrams.

The parameter b^k governs the shrinkage or bonded yield locus and is defined as:

$$b^k = b_0^k \exp(-a |\varepsilon_n^{pk}|) \quad (23)$$

Where, a is an additional parameter describing the reduction of bonding with increasing accumulated normal plastic strain $b^k = |\varepsilon_n^{pk}|$

The resultant hardening law for the preconsolidation pressure on the k^{th} sampling plane may be written as

$$\sigma_{np}^k = \sigma_{np}^{*k} (1 + b^k) \quad (24)$$

In order to avoid the softening strain behaviour, the parameter a should not be over a maximum value

$$a < a_{\max}^k = \frac{1 + b_0^k}{b_0^k (\lambda^* - \kappa^*)} \quad (25)$$

Cudny and Vemeer suggested an alternative parameter a_r defined by the ratio of a and a_{\max}^k

$$a_r = \frac{a}{a_{\max}^k} \quad (26)$$

4. IMPLEMENTATION INTO PLAXIS

The constitutive model was implemented into Plaxis Professional V8.2 using the User defined soil moles module. The strain increments calculated by the program are used to calculate the macro stress state. The micro stresses acting on each sampling plane were, the, calculated by equation (19).

The transformation $T^{\sigma k}$ in equation (19) can be reduced into a form of simplicity in plane strain conditions:

$$T^{\sigma k} = \begin{bmatrix} 0 & 0 & 0 & 0 & -n_2^k & n_1^k \\ -n_1^k n_2^k & n_1^k n_2^k & 0 & -(n_1^k)^2 + (n_2^k)^2 & 0 & 0 \\ (n_1^k)^2 & (n_2^k)^2 & 0 & 2n_1^k n_2^k & 2n_2^k n_3^k & 0 \end{bmatrix} \quad (27)$$

Note that in 2D plane strain analysis, the generation of the vectors $x^{k(1)}$ and $x^{k(2)}$ is not necessary.

With the stress increments, the micro plastic strain on each sampling plane can be easily calculated using equations (18), (19), and (20). The micro plastic strain is then assembled into the global plastic strain using equation 16 to update the macro stresses.

$$\sigma_i = \sigma_i^0 + D_{ij}^{\sigma k} (d\varepsilon_j^{ek} - d\varepsilon_j^{pk}) \quad (28)$$

Where, σ_i, σ_i^0 are previous stresses and current stresses respectively, $d\varepsilon_j^{ek}, d\varepsilon_j^{pk}$ are input strain increment by a program and macro plastic strain calculated by the subroutine respectively.

An important step in this implementation is to control the convergence of the result. The sub-step control was used to control the strain increments given by the program. Usually, the stress increments given by the program are very large, which is in turn can move the stress state too far from the equilibrium condition. Therefore, input strains by the program should be divided into small strain increments in order to warrant the convergence of the iteration process. This sub-step consists of two main tasks: (1) determining the magnitude of the control strain increment and (2) determining the conditions after the sub-step was used i.e. tension stresses appear.

5. CODE CALIBRATION

5.1 Spatial integration framework

A multi-laminate model with Mohr-Coulomb failure criterion was first used to calculate the failure load of a strip footing in undrained/drained conditions assuming weightless soil. In order to obtain the appropriate comparison, only constant elastic modulus was adopted. The following parameters were used:

Undrained condition:
 $E=100000 \text{ kN/m}^3, \nu=0.3, c_u=10\text{KPa}, \psi=0$

Drained condition:
 $E=100000 \text{ kN/m}^3, \nu=0.3, c'=10\text{KPa}, \varphi'=20^\circ, \psi=0$

The resulting failure load for drained condition is in good agreement with the classical Mohr-Coulomb analysis as shown in Figure 5. For undrained condition, the displacements are in good agreement; however, the failure load is different (see Figure 6). This may be

attributed to the fact that failure conditions were not applied simultaneously to all sampling plane. Therefore, soil is able to carry further loads as the failure load is approaching.

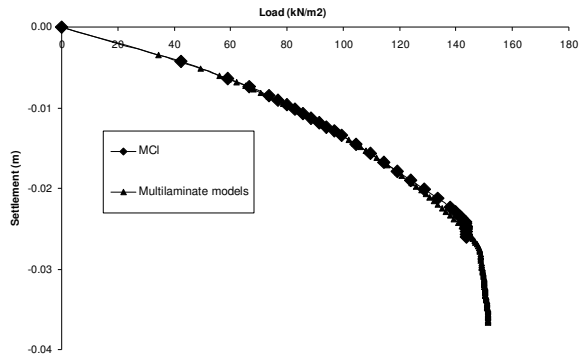


Figure 5. Comparison of load and displacement curve of strip footing in drain condition

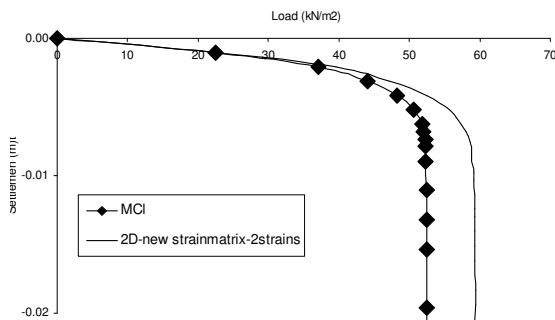


Figure 6. Comparison of load and displacement curve of strip footing in undrained condition

5.2 Effect of model parameters

Analysis was also conducted using the Soft-Soil model (SSM) built into Plaxis. The yield function of the SSM is similar to that of the multilaminate model for $\beta=1$ and bonding affect is not considered.

The multilaminate model is simulated with the following standard and intrinsic parameters:

Standard parameters

$$\varphi' = 20^\circ, c' = 10 \text{ kN/m}^2, \psi = 0^\circ, \nu = \nu_{ur} = 0.2, \kappa^* = 0.02, \lambda^* = 0.1,$$

Intrinsic parameters:

$$\beta = 1, b_0 = 1, \Omega_v = 0.5, a_r = 1$$

It should be noted that Poisson's ratio under unloading-reloading condition is equal to the ratio for normal consolidated to calibrate process with Soft-Soil model is more convenient.

Figure 7 shows the results for the cases of $a_r = 1$, $a_r = 0.75$ while β was kept constant to the model behaviour and

Figure 8 show the influence of parameter β while a_r was kept constant.

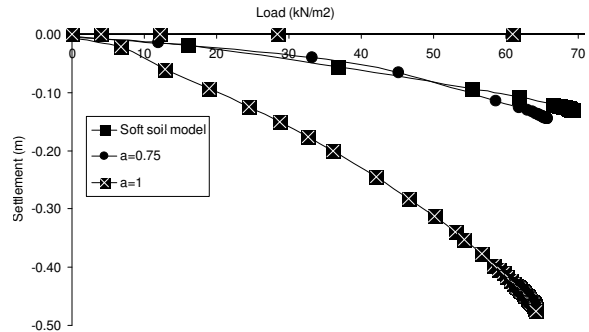


Figure 7. Influence of parameter a_r on the multilaminate model.

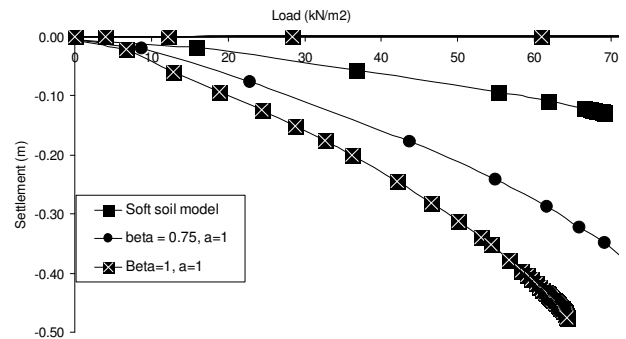


Figure 8. Influence of parameter β while a_r was kept constant.

It was observed that the model response is different from the Soft-Soil model. This may be attributed to some inactive planes that did not expand. A stress state which is still elastic on the macro level may cause plastic strains. On the other hand, a plastic stress state on a macro level may not violate the yield surface. Another reason is related to the question of how reliable the used parameters are.

6. CONCLUSION

The multilaminate model was used to simulate anisotropic clays which were heavily affected by bonding and destructuration phenomenon. These clay characteristics were captured by introducing the bonding parameter to the yield locus on each sampling plane. The model also took into account the anisotropic behaviour of clays by using microstructure tensors simulating the arrangement and interparticle bonding. This constitutive model is simple. It was successfully implemented into the commercial software Plaxis. Further improvement should be carried out such as considering elastic anisotropy and anisotropic strength parameter.

It is also important to be noted that using a sub-step scheme in the numerical implementation is very time-consuming. Implicit integration should be used in each sampling plane to reduce the global iteration and magnitude of each sub step.

7. ACKNOWLEDGEMENTS

This research is supported by the "Fond Québécois de la recherche sur la nature et les technologies" (FQRNT) and a McGill University Research Grant.

REFERENCES

- Anandarajah A, On influence of fabric anisotropy on the stress-strain behavior of clays. *Computers and geotechnics*, Vol. 27, 2000, pp 1-17.
- Cudny M, Vermeer P. A. On the modelling of anisotropy and destructuration of soft clays within the multilaminar framework. *Computer and geotechnics* 31, 2004, pp 1-22.
- Dafalias Y.F, Manzari M.T, Akaishi M, A simple anisotropic clay plasticity model, *Mechanics research communications* Vol. 29, pp 241-245, 2002.
- Fliege J, Maier U. A two-stage approach for computing cubature formulae for the sphere. *Ergebnisberichte Angewandte Mathematik*, University Dortmund 1996. Available from <http://www.mathematik.uni-dortmund.de/lx/research/projects/fliege/nodes/nodes.html>
- Gens A, Nova R. Conceptual bases for a constitutive model for bonded soils and weak rock. *Geotechnical Engineering of hard soils – soft rock*, Anagnostopoulos et al (eds), 1993, pp 485-494.
- Karstunen M, Pande G. N. Strain localization in granular media using multilaminar framework. *Applications of computational mechanics in geotechnical engineering*, Azevedo et al. (eds), 1997
- Karstunen M, Pande G. N. Criterion for strain localization based on multilaminar framework. *Numerical models in geomechanics*, Pietruszczak & Pande (eds), 1997
- Karstunen M. Numerical modelling of strain localization in dense sand. *Acta Polytechnica Scandinavica* No. 113. Espoo. The Finnish Academy of technology 1999.
- Karstunen M, Krenn H, Wheeler S. J, Koskinen M, Zentar R. Effect of anisotropy and destructuration on the behavior of Murro test embankment, *Int. journal of geomechanics*, June 2005, pp. 87-97.
- Kumbhojkar A.S, Banerjee P.K. An anisotropic hardening rule for saturated clays. *Int. journal of plasticity*, Vol. 9, pp 861-888, 1993
- Leroueil S, Vaughan P.R, The general and congruent effects of structure in natural soils and weak rocks, *Geotechnique*, 40, pp 467-488, 1990.
- Neher, H. P, Cudny M, Wiltafsky C, Schweiger H.F. Modelling principal stress rotation effects with multilaminar type constitutive models for clay. In: *Numerical models in Geomechanics – NUMOG VIII*, Rome, p. 41-7
- Pande G. N, Sharma K. G. Multi-laminar model of clays – A numerical evaluation of the influence of rotation of the principal stress axes. *Int. journal for numerical and analytical methods in geomechanics*, 1983; Vol. 7, pp 397-418
- Pande G.N, Yamada M. The multilaminar framework of models for rock and soil masses. *Applications of computational mechanics in geotechnical engineering*, Vargas et al (eds), 1994
- Pietruszczak S, Pande G. N. Multi-laminar framework of soil models – Plasticity formulation. *Int. journal for numerical and analytical methods in geomechanics*, 1987; Vol. 11, pp 651-658.
- Pietruszczak S, Pande G. N. Description of soil anisotropy based on multi-laminar framework. *Int. journal for numerical and analytical methods in geomechanics*, 2001; Vol. 25, pp 197-206
- Pietruszczak S, Mroz Z. On failure criteria for anisotropic cohesive-frictional materials. *Int. journal for numerical and analytical methods in geomechanics*, 2001; Vol. 25, pp 509-524
- Schuller H, Schweiger H. F. Application of a multilaminar model to simulation of shear band formation in NATM-tunnelling. *Computer and geotechnics* 29, 2002, pp 501-524
- Su S. F, Liao H. J, Lin Y. H. Base stability of deep excavation in anisotropic soft clay. *Journal of geotechnical and geoenvironmental engineering*, Sept. 1998, pp. 809-819
- Sun D.A, Matsuoka H, Yao Y.P, Ishii H, An anisotropic hardening elastoplastic model for clays and sands and its application to FE analysis, *Computer and Geotechnics* 31, pp 37-46, 2004.
- Wheeler S.J, Cudny M, Neher H.P, Wiltafsky C. Some developments in constitutive modelling of soft clays. *Int. workshop on geomechanics of soft soils – Theory and Practice*. Veermeer, Schweiger, Karstunen & Cudny (eds), 2003.
- Wiltafsky C, Messerklinger S, Schweiger H.F. An advanced multilaminar model for clay. *Numerical models in geomechanics, NUMOG VIII*, Pande & Pietruszczak (eds), 2002.
- Wood D. M, Soil behavior and Critical state soil mechanics, Cambridge University Press, Cambridge, 1990
- Wood, D. M, Graham J. Anisotropic elasticity and yielding of a natural plastic clay, *Int. Journal of plasticity*, Vol. 6, pp377-388, 1990